



Annual hydrographic variability in Antarctic coastal waters infused with glacial inflow

Maria Osińska¹, Kornelia A. Wójcik-Długoborska², Robert J. Bialik²

¹Institute of Oceanography, University of Gdańsk, Piłsudskiego 46, 81-378 Gdynia, Poland

5 ² Institute of Biochemistry and Biophysics, Polish Academy of Sciences, Pawińskiego 5a, 02-106 Warsaw, Poland

Correspondence to: Robert J. Bialik (rbialik@ibb.waw.pl)

Abstract.

During the thirty-eight months between December 2018 and January 2022, multiparameter hydrographic measurements were taken at thirty-one sites within Admiralty Bay, King George Island, Antarctica. These records consisted of water column
10 measurements (down to 100 m) of temperature, conductivity, turbidity, and pH as well as the dissolved oxygen, dissolved organic matter, chlorophyll A and phycoerythrin contents. The sites were chosen due to their variable distances from glacial fronts and open ocean waters. Fifteen sites were localized within smaller glacial coves, with waters highly impacted by glacial infusions; seven sites were located in the open waters of the main body of Admiralty Bay; and nine were located in intermediate conditions of the Ezcurra Inlet. The final dataset consists of measurements carried out over 142 separate days, with an average
15 3.74 measurements per month. However, data were not collected regularly throughout the year and were collected less frequently during winter, though data were gathered for all but two winter months. On average, each site was investigated 98.2 times. Due to calibration issues, absolute values of optically measured properties occasionally show impossible negative values, but the relative distributions of these values remain valid. Variabilities in the measured properties each season and throughout the whole duration of the project reveal regular oscillations as well as possible long-term trends.

20 1 Introduction

Fjords and bays mixed with waters from glacial outflow are unique environments that are vital for maintaining polar ecosystems and, considering their size, are critical regions of the global ocean. When freshwater from glaciers is introduced into marine environments, the combination of water masses alter the properties of the seawater, forming glacially modified water (GMW) (Straneo, 2012). This alteration of the ocean's water chemistry has far reaching effects that have been
25 investigated in numerous studies across a diversity of fields. GMW influences the hydrodynamics and thermodynamics of the ocean (Bendtsen et al., 2015; Chauché et al., 2014), changes the ocean's chemical composition (Kanna et al., 2020; Fransson et al., 2015) and impacts ecosystems both directly and indirectly (Gerringa et al., 2012; Oliver et al., 2018). Therefore, there



are significant justifications to investigate water quality properties in glacial bays and fjords and to track their variability to potentially predict future changes.

30 The majority of studies examining the influence of GMW on seawater have been performed in the Northern Hemisphere. Some notable works in this field have been performed in the Antarctic region (among others: Cape et al., 2019; Forsch et al., 2021; Meredith et al., 2018; Monien et al., 2017; Schloss et al., 2014); nevertheless, widely available data that describe water quality in glacial bays beyond seasonal timescales, at high sampling resolutions, and that examine multiple variables remains non-existent. In fact, such datasets are scarce for the Arctic and Alaska as well.

35 To address this deficiency, an intricate investigation campaign was designed with the intention of comprehensively observing the seasonal oscillations and long-term trends in water quality variability of Admiralty Bay (AB), King George Island in Western Antarctica. The goal of this project was to widen the scope of previously gathered observations by expanding the overall duration of monitoring, increasing the frequency and number of measured parameters and to acquire data across all seasons of the year.

40 **2 Research Area**

AB is a 177.04 km² cove southeast of King George Island, the largest island of the Southern Shetlands in Western Antarctica. In its interior, AB is subdivided into three distinct areas: Ezcurra, Mackellar and Martel Inlets, which all blend together approximately 11 km from the open ocean waters of the Bransfield Strait, forming the main body of AB (Figure 1). Its coastline has a length of 150 km, of which 102 km consist of rocky coastline and the remaining 38 km consist of ice-water boundaries
45 (Figure 1, yellow lines (Gerrish et al., 2021)). The tidewater glaciers that form these frontiers are the outer regions of two large icefields, the Warsaw and Krakow Icefields. Both icefields are reportedly experiencing unprecedented transformation due to the effects of climate warming (Rückamp et al., 2010; Dziembowski and Bialik, 2022) and are draining into AB through numerous glacial creeks.

To summarize this dataset, it was decided to distinguish different zones within AB to recognize distinctions in water properties
50 that were dependent on proximity to the glacial fronts and open ocean waters. Three zones have been assigned:

- Glacial coves: Distinct smaller bays formed near tidewater glaciers in which marine waters are under the direct influence of glacial meltwater input. Here, three glacial coves were analysed in depth, the cove near Lange Glacier (1.50 km² in area with a 2.81 km long ice-water frontline), Spera Cove (2.45 km² in area with a 4.33 km long ice-water frontline) near Vieville Glacier and Suszczewski Cove near Ecology Glacier (0.69 km² in area with a 0.36 km
55 long ice-water frontline). All three of these basins are undergoing long-term transformation caused by continuously moving and developing glacial fronts. This is visualized in Figure 1, where the light blue line on the glacial cove insets represents the ice-water boundary in 2018 (based on a Sentinel satellite image from Mar 10th, 2018), which is different from the frontline shown on a satellite picture presented in Figure 1 taken in December of 2021 (Sentinel,



60 Dec 29, 2021). The change is especially noticeable in Spera Cove near Vieville glacier, where the ice front has retreated 500 m within three years in some locations.

- Main body of Admiralty Bay: Open bay waters in the main body of the cove, most directly influenced by the open ocean waters of the Bransfield Strait with which it is connected by a 13.45 km wide outlet. Nevertheless, this location is also affected by glacial input, especially in its northern parts.
- Ezcurra Inlet (area of 21.32 km²): This is an intermediate area separated from Admiralty Bay waters by a relatively narrow passage (2.40 km wide) and influenced by the surrounding ice coastline (9.58 km long of 32.67 km long coastline).

70 These areas are shown in Figure 1 and are used as separate, but deeply interrelated, regions for further study. To that end, measurement points were chosen, whose localizations are marked on the map in Figure 1, and their details (location, depth, number of measurements performed at a given point, and, in the case of glacial cove points, distance from the water-ice boundary) are summarized in Table 1.

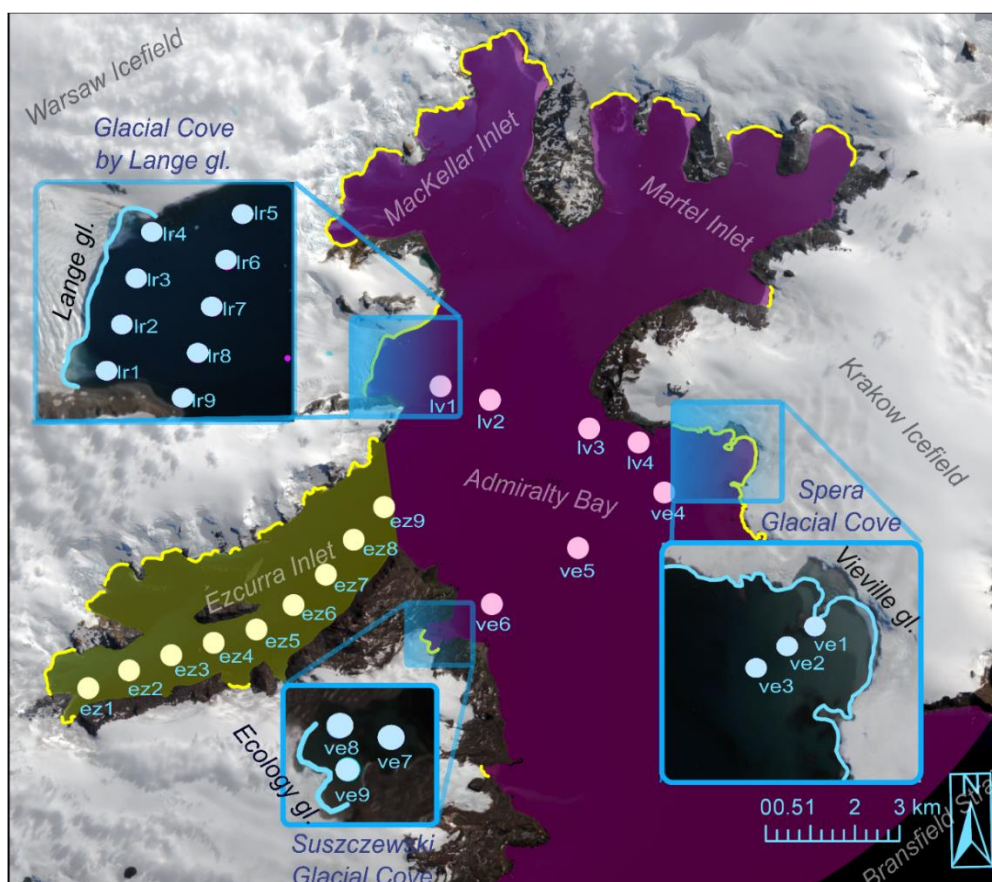


Figure 1: Map of Admiralty Bay with measurement points in three distinct zones: main Admiralty Bay (pink), Glacial coves (blue inset boxes) and Ezcurra Inlet (yellow lines based upon Gerrish et al., 2021). Bright yellow shows current position of the ice-water coastline, in bright blue insets the position of the coastline on Mar 10th, 2018. Source: Sentinel imagery, Dec 29th, 2021.



75 **Table 1: Details of the measurement sites**

site name and zone	latitude	longitude	depth (m)	distance from glacial front (m) (2018-2021)
Glacial Coves				
lr1	-58.4892	-62.1227	19	315-322
lr2	-58.4868	-62.1195	>100	266-330
lr3	-58.4845	-62.1163	>100	275-332
lr4	-58.4821	-62.1131	23	260-343
lr5	-58.4687	-62.1120	8	940-1018
lr6	-58.4711	-62.1152	66	880-951
lr7	-58.4734	-62.1184	>100	902-952
lr8	-58.4758	-62.1216	>100	868-912
lr9	-58.4782	-62.1247	3	929-932
ve1	-58.3380	-62.1361	2	71-481
ve2	-58.3429	-62.1375	8	359-780
ve3	-58.3483	-62.1391	29	686-1118
ve7	-58.4613	-62.1716	4	455-469
ve8	-58.4677	-62.1709	2	210-232
ve9	-58.4668	-62.1734	3	113-128
Admiralty Bay				
lv1	-58.4624	-62.1221	>100	
lv2	-58.4412	-62.1251	>100	
lv3	-58.3989	-62.1313	71	
lv4	-58.3777	-62.1343	17	
ve4	-58.3671	-62.1445	58	
ve5	-58.4047	-62.1553	>100	
ve6	-58.4424	-62.1662	55	
Ezcurra Inlet				
ez1	-58.6172	-62.1812	56	
ez2	-58.5994	-62.1778	67	
ez3	-58.5811	-62.1750	51	
ez4	-58.5626	-62.1727	61	
ez5	-58.5441	-62.1702	68	
ez6	-58.5279	-62.1655	84	
ez7	-58.5136	-62.1595	>100	
ez8	-58.5012	-62.1526	>100	



ez9 | -58.4878 -62.1462 >100

Measurements in Glacial Coves and Admiralty Bay were taken from December 2018 until January 2022 and in Ezcurra Inlet from October 2019 till January 2022.

3 Methodology

80 3.1 Measured water properties

Measurements were performed with two professional YSI multiparameter EXO sondes (EXO1 and EXO2), designed for simultaneous investigation of multiple water quality properties, used and tested by researchers worldwide (Snazelle, 2015). EXO1 consists of five sensor ports and EXO2 contains seven ports; therefore, the water properties measured varied between the particular campaigns. Of the 3045 measurements collected, 2069 were acquired using the EXO1 sonde, and the remaining
 85 976 were acquired with EXO2 and its larger sensor capacity (details seen in Figure 2).

The list of sensors and properties investigated by them is summarized in Table 2. Some hydrographic properties are derived indirectly from the direct measurements of other water column properties. In these cases, the sondes automatically calculated the additional related values based on universally accepted formulas. For example, salinity was calculated based on conductivity and temperature measurements (for details see YSI manual (YSI Inc, 2017)).

90 **Table 2. List of sensors and measured water properties (based upon (YSI Inc, 2017))**

Sensor		Measured property	Unit	Accuracy/linearity	
EXO2	EXO1	Conductivity/Temperature	Conductivity	$\mu\text{S/cm}$	0-100 mS/cm: $\pm 0.5\%$ of reading or 0.001 mS/cm, whichever is greater; 100-200 mS/cm: $\pm 1\%$ of reading
			Specific Conductivity	$\mu\text{S/cm}$	
			nLF Conductivity	$\mu\text{S/cm}$	
			Salinity	PSU	
			Temperature	$^{\circ}\text{C}$	
		Depth and Level	Pressure	PSI	± 0.04 m
		Depth	m		
		Dissolved Oxygen	Dissolved Oxygen	mg/L	± 0.01 mg/L
			Dissolved Oxygen Saturation	%	
			Local Saturation	%	
	pH	pH	-, mV	± 0.01	



		Turbidity	Turbidity	FNU	0.3 FNU or $\pm 2\%$ of reading, whichever is greater
not measured by EXO1		fDOM	Dissolved Organic Matter	QSU, RFU	$R^2 > 0.999$ for serial dilution of 300 ppb Quinine Sulphate solution
		Total Algae (Chl & BGA)	Chlorophyll A	$\mu\text{g/L}$, RFU	$R^2 > 0.999$ for serial dilution of Rhodamine WT solution from 0-400 $\mu\text{g/L}$ Chl equivalents
			BGA (Phycoerythrin)	PE $\mu\text{g/L}$, RFU	$R^2 > 0.999$ for serial dilution of Rhodamine WT solution from 0-280 $\mu\text{g/L}$ PE equivalents

3.2 Measurement procedure and sources of possible data errors and missing values

Measurements were conducted from the deck of the Zodiac boat (Figure 2). When the boat was in the designated point, the sonde lowered by the cable from the reel to a maximum depth of 100 m. At sites where the depth surpasses 100 m, the cable was fully deployed, and at shallower points, the instruments was lowered until the depth indicator on the handheld device stabilized. This shows the limitation of this study as data was not obtained from bottom portions of the water column, particularly in the central part of the bay (see Table 1 for information on which sites bottom layers have not been investigated). The sampling rate of the sondes were initially 0.2 Hz up to December 30th, 2019, when the sampling frequency increased to 1 Hz.

The intended descent rate of the instrument was 1 m per second, but since this was manually controlled by the research personnel, the descent rate of the sonde varied significantly. Furthermore, the fact that the measurements were acquired by different crews may cause some discrepancy in the acquired data. The sensitivity of particular sensors varied, meaning that if the probe was lowered too quickly the measurements taken by some sondes may incorrectly correlate with the depth attributed to those measurements.

Other obstacles were caused by challenging weather and sea conditions. Often, waving and surface currents considerably influenced the position of the boat, making it impossible to remain stationed at the assigned site location for the duration the cast. This can be seen by position data recorded via handheld GPS during sensor deployment and included within the data file. Currents below the surface moved the sonde and cable horizontally from the initial cast position by an unknown extent.

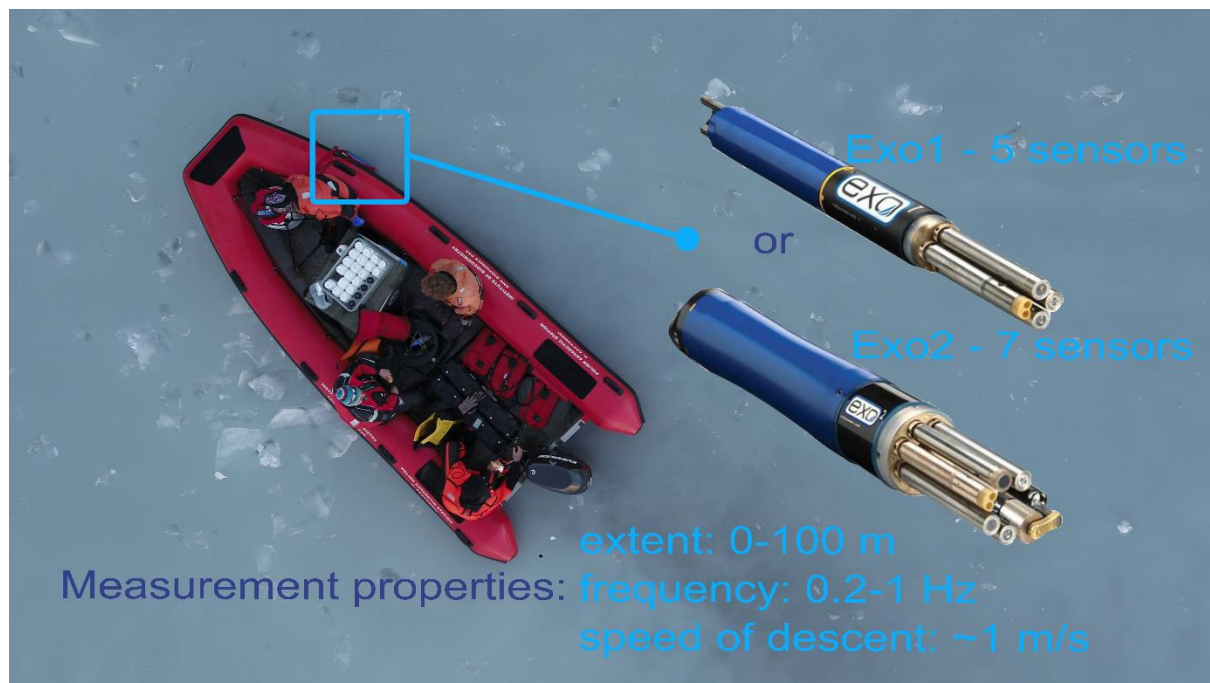


110 On numerous occasions ice prevented scientists from reaching specific sites. This was frequently the case in areas close to glacial fronts, most notably when the water surface froze during winter months and when glacial calving increased in the summer.

All of the sensors were calibrated in accordance with guidelines found in the YSI EXO Manual (YSI Inc, 2017) and replaced after the appropriate time or when malfunctions occurred that could not be otherwise resolved. The depth/pressure level sensor was calibrated at the start of every survey day.

115 Optical sensors for turbidity, total algae and fDOM were calibrated using deionized water. However, the correct standards occasionally showed negative values. This was particularly frequent for measurements of phytoplankton pigments. These values have been left intact in the data file since they represent the correct variability of these properties; however, their absolute values should be considered carefully, and more attention should be given to the relative units (RFU) for chlorophyll A, phycoerythrin and fDOM. Turbidity FNU values have been confirmed in Admiralty Bay waters through the laboratory
120 procedure explained in detail by Wójcik-Długoborska et al. (2022).

Finally, after basic data analysis, some extreme outlier data, most likely caused by incidental crew mistakes or temporary sonde malfunctions, were manually removed from the final dataset.

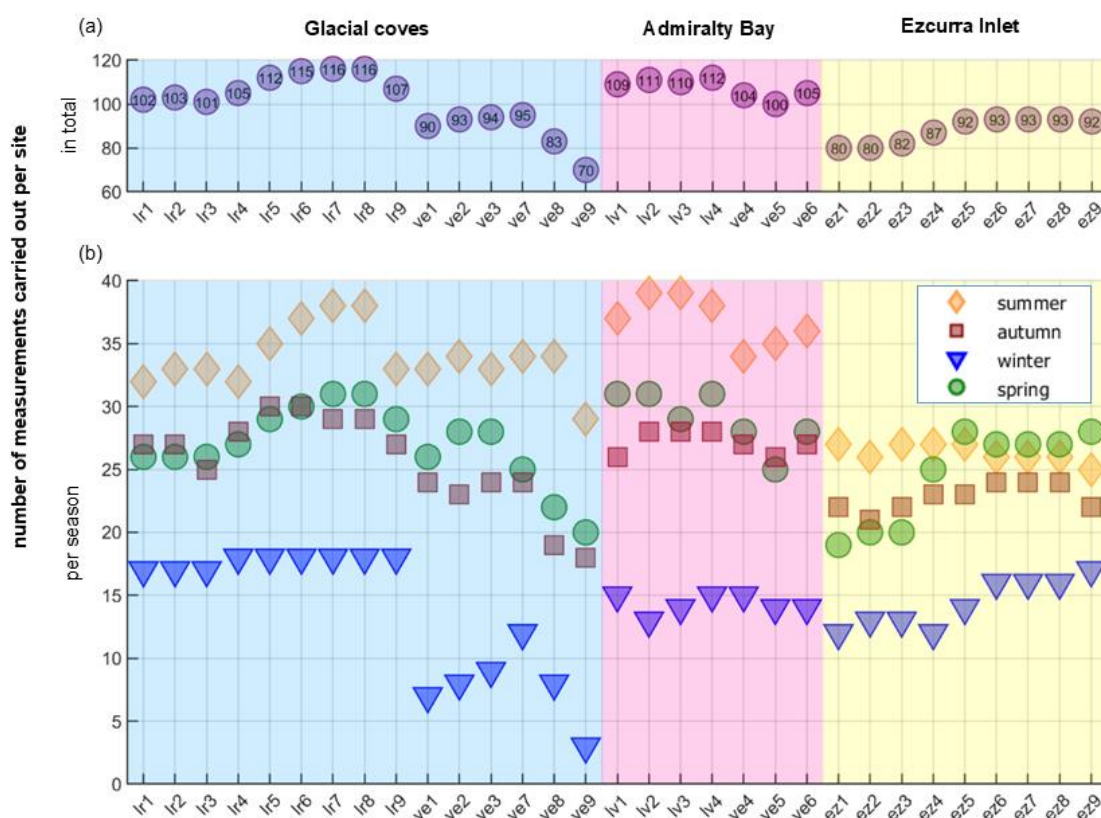


125 **Figure 2. Measurements visualisation, used sondes and measurement properties. In the background scientists in Zodiac boat during measurements of water properties visibly infused with turbid GMW (source of sonde close-ups: <https://observer.com/products/ysi-exo-series-multiparameter-sonde/>)**



4 Results

The results of the measurement campaign discussed above consist of a large and complex dataset describing the variability of the physical, chemical and biological properties in glacially influenced bays. Figure 3 presents a summary of the total number of investigations performed. This shows that even at the sites sampled the least, it was possible to gather data during all seasons. However, most studies were performed during summer across all zones, while the fewest measurements were collected in winter. Interestingly, despite the unpredictable conditions in the Glacial coves, the number of surveys at each site fluctuates around one hundred per location (average 98.2 measurements per site), which is promising for future statistical analysis.

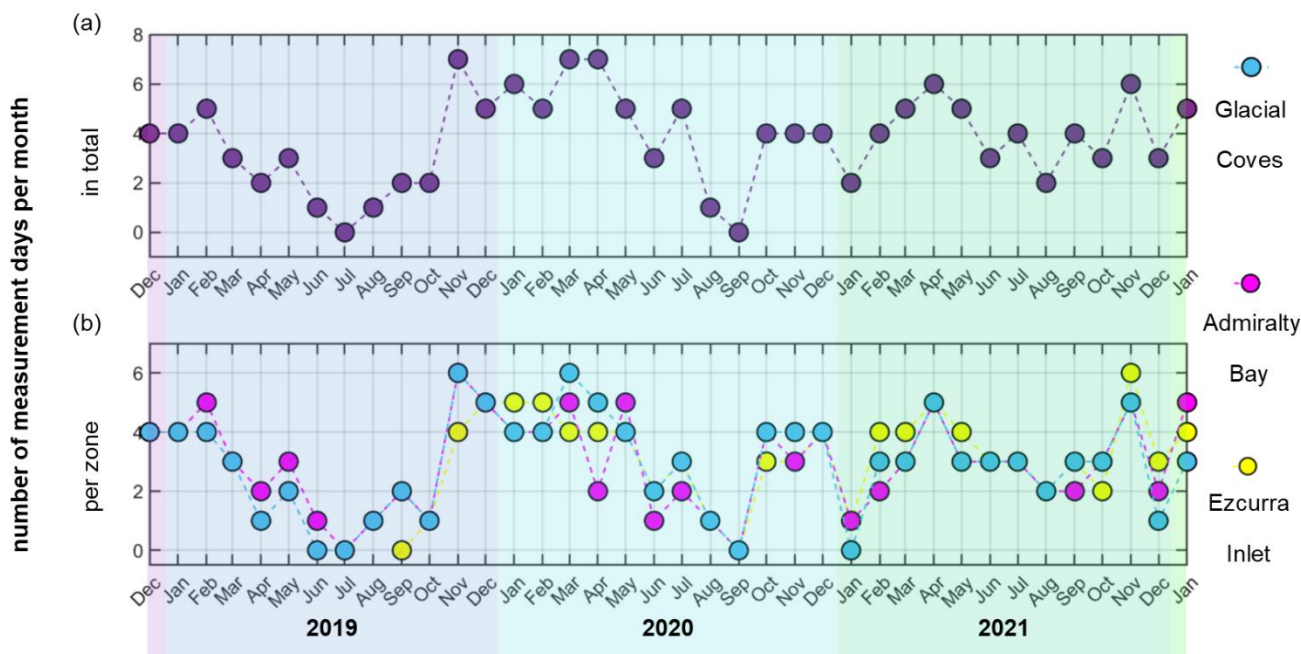


135 **Figure 3. Number of measurements taken at the designated sites in total (a) and by season (calendar) (b) in the period from December 2018 until January 2022**

Considering the complete duration of the projects (see Figure 4), it is noticeable how the number of measurement days fluctuated, with increases during the warmer seasons where there was a maximum of seven measurement days per month. In Figure 4(b), we observe that the same tendencies apply to all the zones, and none of them have been more frequently investigated to any degree of significance. The average number of measurements per month was 3.74 in the Glacial coves and



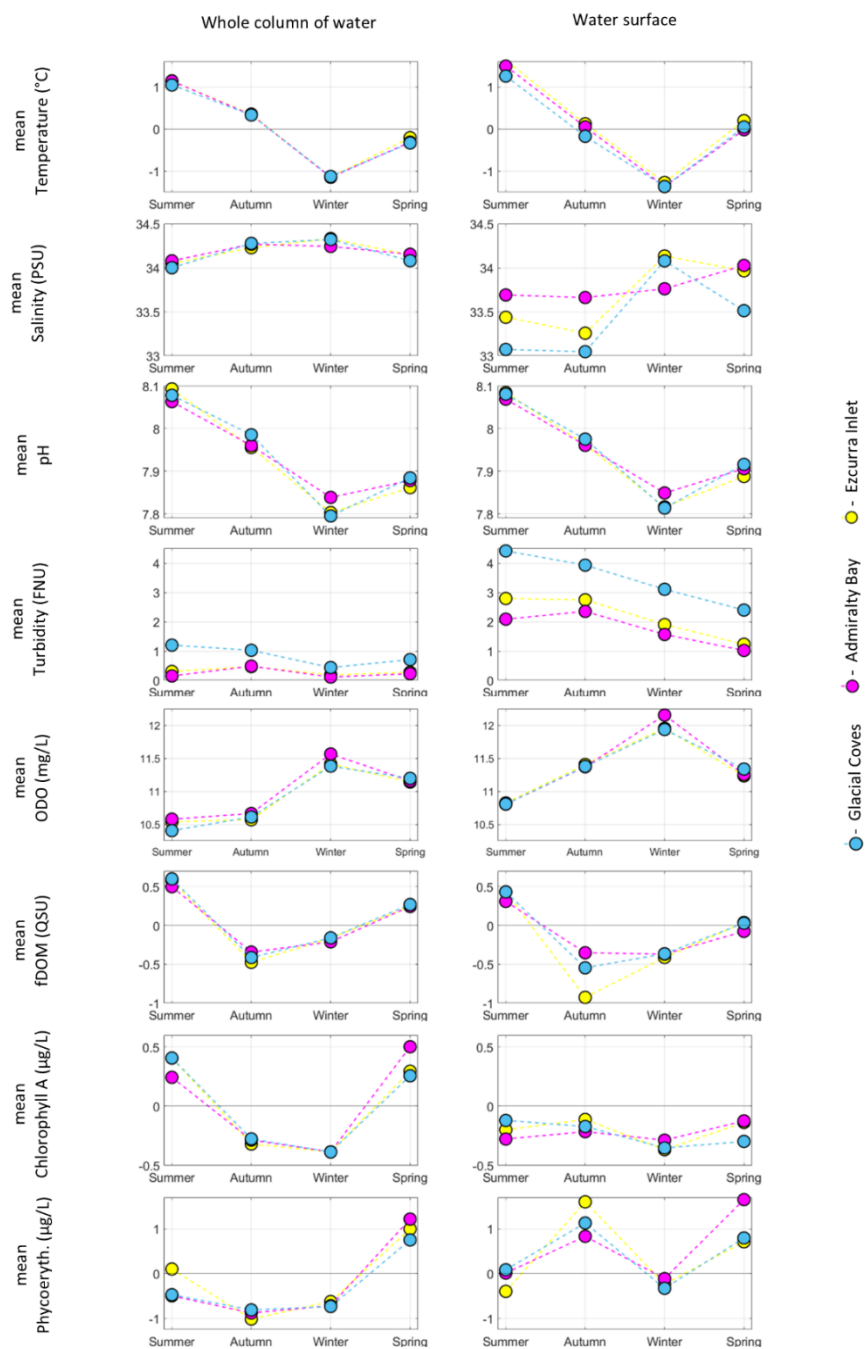
2.91 in Admiralty Bay, with the same number of successful measurement days (111) throughout the whole duration of the project, and 2.42 for Ezcurra Inlet over 92 measurement days.



145 **Figure 4. Number of measurement days per month, (a) in total and (b) per each zone (counted days in which measurements in at least half of zone sites have been performed)**

The division of sites into three zones shows how proximity to glacial fronts and open ocean waters alters particular water quality properties. This effect is also notably correlated with seasonal shifts (Figure 5). Figure 5 illustrates how different properties vary in surface layers in contrast with the whole column of water (limited to 100 m of depth). This shows the impact of both atmospheric forcing and glacial outflow, which, based on buoyant plume model theory (Kimura et al., 2014; Mankoff et al., 2016; Jenkins, 2011) and observations (Chauché et al., 2014; Osińska et al., 2021), is mainly contained in the top layer of the ocean. Therefore, the results provide information on seasonal changes in water properties and glacial-ocean interactions and can be used for validation of previously formulated methods of GMW tracking.

150 The measured mean values of fDOM, chlorophyll A and phycoerythrin during autumn and winter are negative, which demonstrates imperfections of this methodology and is due to incorrect calibration of the sensors used. This is also true for the turbidity mean monthly values shown in Figure 6. However, in Figures 5 and 6, the overall relative distribution of these parameters is in accordance with expectations, with low values for all of them seen during colder months and with turbid waters seen specifically in the top layers of the water and closer to glacial fronts. This proves the validity of hydrographic measurements as a representation of relative variability but not for information on their absolute values.

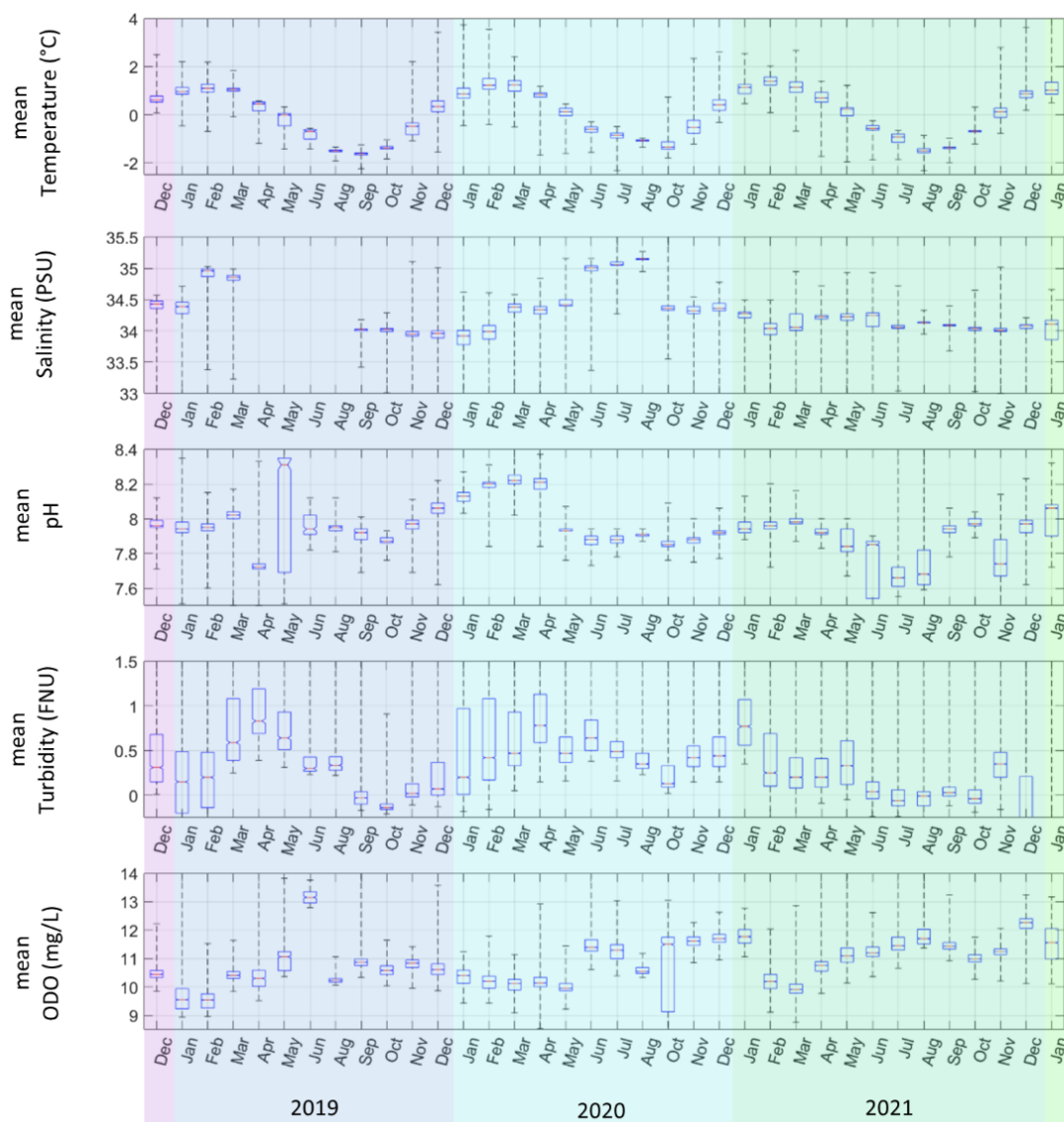


160

Figure 5: Mean values of measured properties dependent on season, divided into the whole column of water and the top 5 m of surface water.



The 38-month-long duration of the project allowed for the tracking of seasonal variability across all measured hydrographic properties and showed consistency in all cases (Figure 6). Moreover, this duration permits cautious predictions regarding long-term shifts in water column properties and reveals the impact of climate change or other influential conditions in this region. Using more sophisticated techniques, it is possible to more precisely determine the nature of this variability. The quantities of chlorophyll A, phycoerythrin and fDOM are not presented in Figure 6 since their measurement was significantly less frequent.



170 **Figure 6.** Boxplot of monthly properties' mean values (excluding properties measured solely by EXO2 sonde due to their significantly shorter timeseries).



5 Data availability

Described dataset is freely accessible at the Pangea repository via following doi:
<https://doi.pangaea.de/10.1594/PANGAEA.947909> (Osińska et al., 2022), under a non-restrictive license CC BY 4.0. (at this
moment doi is yet inactive since the editing process in Pangea is still taking place, so for reviewing purposes please use
175 following link: <https://www.pangaea.de/tok/068391f63c6567f178b401bcdac7ae3d3134b625>).

6 Conclusions

The assembled dataset shared here presents an opportunity for a better understanding of Admiralty Bay water characteristics
over the 38-month survey period and can be used in further studies exploring the nature and changes in glacially influenced
regions in general. The measurement technique was not perfect since some optically measured parameters showed negative
180 values at times. However, the sheer magnitude of this investigation is validated by the 3045 separate measurements acquired
on 142 separate days over 38 months and inspires optimism regarding future work and application of this data.

The scope of measured parameters (thermodynamic, physical, chemical and biological) paints a wide and precise picture of
AB hydrographic variability during all months of the year and may allow for a multidisciplinary analysis of the complex
processes that take place in this location. The varied settings of study sites allow for the tracking and identification of GMW
185 and other water masses (Straneo et al., 2011; Chauché et al., 2014). Additionally, this sizable dataset can be used as a tool for
better understanding the general hydrodynamics and thermodynamics of glacial bays and fjords and may be employed for the
validation of coupled glacier-ocean modelling (Cowton et al., 2015; De Andrés et al., 2021; Bertino and Holland, 2017).

Author Contribution

MO – conceptualization, data curation, formal analysis, investigation, methodology, validation, visualization and writing
190 (original draft preparation), KAW – investigation, methodology and writing (review & editing); RJB – funding acquisition,
investigation, project administration, resources, supervision and writing (review & editing)

Competing interests

The authors declare that they have no conflict of interest.

Acknowledgments

195 This work was supported by the National Science Centre, Poland, Grant No. UMO-2017/25/B/ST10/02092 ‘Quantitative
assessment of sediment transport from glaciers of South Shetland Islands on the basis of selected remote sensing methods’.



Calculations were made possible by software provided by CI TASK (Center of the Tri-City Academic Computer Network) in Gdańsk. Special credits are owed to all invincible members of so called MorMon team, part of Polish Antarctic Station's crew, that throughout whole period of the project, in often trying and almost always uncomfortable conditions carried out presented measurements.

References

- De Andrés, E., Otero, J., Navarro, F. J., and Walczowski, W.: Glacier-plume or glacier-fjord circulation models? A 2-D comparison for Hansbreen-Hansbukta system, Svalbard, *J. Glaciol.*, 67, 797–810, <https://doi.org/10.1017/jog.2021.27>, 2021.
- Bendtsen, J., Mortensen, J., Lennert, K., and Rysgaard, S.: Heat sources for glacial ice melt in a west Greenland tidewater outlet glacier fjord: The role of subglacial freshwater discharge, *Geophys. Res. Lett.*, 42, 4089–4095, <https://doi.org/10.1002/2015GL063846>, 2015.
- Bertino, L. and Holland, M. M.: Coupled ice-ocean modeling and predictions, *J. Mar. Res.*, 75, 839–875, <https://doi.org/10.1357/002224017823524017>, 2017.
- Cape, M. R., Vernet, M., Pettit, E. C., Wellner, J., Truffer, M., Akie, G., Domack, E., Leventer, A., Smith, C. R., and Huber, B. A.: Circumpolar deep water impacts glacial meltwater export and coastal biogeochemical cycling along the west Antarctic Peninsula, *Front. Mar. Sci.*, 6, 144, <https://doi.org/10.3389/FMARS.2019.00144/BIBTEX>, 2019.
- Chauché, N., Hubbard, A., Gascard, J. C., Box, J. E., Bates, R., Koppes, M., Sole, A., Christoffersen, P., and Patton, H.: Ice-ocean interaction and calving front morphology at two west Greenland tidewater outlet glaciers, *Cryosphere*, 8, 1457–1468, <https://doi.org/10.5194/tc-8-1457-2014>, 2014.
- Cowton, T., Slater, D., Sole, A., Goldberg, D., and Nienow, P.: Modeling the impact of glacial runoff on fjord circulation and submarine melt rate using a new subgrid-scale parameterization for glacial plumes, *J. Geophys. Res. Ocean.*, 120, 796–812, <https://doi.org/10.1002/2014JC010324>, 2015.
- Dziembowski, M. and Bialik, R. J.: The Remotely and Directly Obtained Results of Glaciological Studies on King George Island: A Review, *Remote Sens.*, 14, 2736, <https://doi.org/10.3390/RS14122736>, 2022.
- Forsch, K. O., Hahn-Woernle, L., Sherrell, R. M., Rocanova, V. J., Bu, K., Burdige, D., Vernet, M., and Barbeau, K. A.: Seasonal dispersal of fjord meltwaters as an important source of iron and manganese to coastal Antarctic phytoplankton, *Biogeosciences*, 18, 6349–6375, <https://doi.org/10.5194/BG-18-6349-2021>, 2021.
- Fransson, A., Chierici, M., Nomura, D., Granskog, M. A., Kristiansen, S., Martma, T., and Nehrke, G.: Effect of glacial drainage water on the CO₂ system and ocean acidification state in an Arctic tidewater-glacier fjord during two contrasting years, *J. Geophys. Res. Ocean.*, 120, 2413–2429, <https://doi.org/10.1002/2014JC010320>, 2015.
- Gerringa, L. J. J. A., Alderkamp, A.-C. C., Laan, P., Thuróczy, C.-E., De Baar, H. J. J. W., Mills, M. M., van Dijken, G. L., van Haren, H., Arrigo, K. R., Thuróczy, C. E., De Baar, H. J. J. W., Mills, M. M., van Dijken, G. L., Haren, H. van, and Arrigo,



- K. R.: Iron from melting glaciers fuels the phytoplankton blooms in Amundsen Sea (Southern Ocean): Iron biogeochemistry, *Deep. Res. Part II Top. Stud. Oceanogr.*, 71–76, 16–31, <https://doi.org/10.1016/j.dsr2.2012.03.007>, 2012.
- 230 Gerrish, L., Fretwell, P., and Cooper, P.: High resolution vector polylines of the Antarctic coastline (7.4) [Data set], <https://doi.org/https://doi.org/10.5285/e46be5bc-ef8e-4fd5-967b-92863fbe2835>, 2021.
- Jenkins, A.: Convection-Driven Melting near the Grounding Lines of Ice Shelves and Tidewater Glaciers, *J. Phys. Oceanogr.*, 41, 2279–2294, <https://doi.org/10.1175/JPO-D-11-03.1>, 2011.
- Kanna, N., Sugiyama, S., Fukamachi, Y., Nomura, D., and Nishioka, J.: Iron Supply by Subglacial Discharge Into a Fjord
235 Near the Front of a Marine-Terminating Glacier in Northwestern Greenland, *Global Biogeochem. Cycles*, 34, <https://doi.org/10.1029/2020GB006567>, 2020.
- Kimura, S., Holland, P. R., Jenkins, A., and Piggott, M.: The Effect of Meltwater Plumes on the Melting of a Vertical Glacier Face, *J. Phys. Oceanogr.*, 44, 3099–3117, <https://doi.org/10.1175/JPO-D-13-0219.1>, 2014.
- Mankoff, K. D., Straneo, F., Cenedese, C., Das, S. B., Richards, C. G., and Singh, H.: Structure and dynamics of a subglacial
240 discharge plume in a Greenlandic fjord, *J. Geophys. Res. Ocean.*, <https://doi.org/10.1002/2016JC011764>, 2016.
- Meredith, M. P., Falk, U., Bers, A. V., Mackensen, A., Schloss, I. R., Barlett, E. R., Jerosch, K., Busso, A. S., and Abele, D.: Anatomy of a glacial meltwater discharge event in an Antarctic cove, *Philos. Trans. R. Soc. A Math. Phys. Eng. Sci.*, 376, <https://doi.org/10.1098/rsta.2017.0163>, 2018.
- Monien, D., Monien, P., Brünjes, R., Widmer, T., Kappenberg, A., Silva Busso, A. A., Schnetger, B., and Brumsack, H. J.:
245 Meltwater as a source of potentially bioavailable iron to Antarctica waters, *Antarct. Sci.*, 29, 277–291, <https://doi.org/10.1017/S095410201600064X>, 2017.
- Oliver, H., Luo, H., Castelao, R. M., van Dijken, G. L., Mattingly, K. S., Rosen, J. J., Mote, T. L., Arrigo, K. R., Rennermalm, Å. K., Tedesco, M., and Yager, P. L.: Exploring the Potential Impact of Greenland Meltwater on Stratification, Photosynthetically Active Radiation, and Primary Production in the Labrador Sea, *J. Geophys. Res. Ocean.*, 123, 2570–2591,
250 <https://doi.org/10.1002/2018JC013802>, 2018.
- Osińska, M., Bialik, R. J., and Wójcik-Długoborska, K. A.: Interrelation of quality parameters of surface waters in five tidewater glacier coves of King George Island, Antarctica, *Sci. Total Environ.*, 771, 144780, <https://doi.org/10.1016/j.scitotenv.2020.144780>, 2021.
- Osińska, M., Wójcik-Długoborska, K. A., and Bialik, R. J.: Water conductivity, salinity, temperature, turbidity, pH, fluorescent
255 dissolved organic matter (fDOM), optical dissolved oxygen (ODO), chlorophyll a and phycoerythrin measurements in Admiralty Bay, King George Island, from Dec 2018 to Jan 2022, *PANGAEA*, <https://doi.org/10.1594/PANGAEA.947909>, 2022.
- Rückamp, M., Blindow, N., Suckro, S., Braun, M., and Humbert, A.: Dynamics of the ice cap on King George Island, antarctica: Field measurements and numerical simulations, *Ann. Glaciol.*, 51, 80–90,
260 <https://doi.org/10.3189/172756410791392817>, 2010.



- Schloss, I. R., Wasilowska, A., Dumont, D., Almandoz, G. O., Hernando, M. P., Michaud-Tremblay, C. A., Saravia, L., Rzepecki, M., Monien, P., Monien, D., Kopczyńska, E. E., Bers, A. V., and Ferreyra, G. A.: On the phytoplankton bloom in coastal waters of southern King George Island (Antarctica) in January 2010: An exceptional feature?, *Limnol. Oceanogr.*, 59, 195–210, <https://doi.org/10.4319/lo.2014.59.1.0195>, 2014.
- 265 Snazelle, T. T.: Evaluation of Xylem EXO water-quality sondes and sensors, Open-File Rep., <https://doi.org/10.3133/OFR20151063>, 2015.
- Straneo, F.: Impact of the large scale ocean circulation on Greenland’s outlet glaciers, *Quat. Int.*, 279–280, 472, <https://doi.org/10.1016/j.quaint.2012.08.1584>, 2012.
- 270 Straneo, F., Curry, R. G., Sutherland, D. A., Hamilton, G. S., Cenedese, C., Våge, K., and Stearns, L. A.: Impact of fjord dynamics and glacial runoff on the circulation near Helheim Glacier, *Nat. Geosci.*, 4, 322–327, <https://doi.org/10.1038/ngeo1109>, 2011.
- Wojcik-Dugoborska, K. A., Osinska, M., and Bialik, R. J.: The impact of glacial suspension color on the relationship between its properties and marine water spectral reflectance, *IEEE J. Sel. Top. Appl. Earth Obs. Remote Sens.*, <https://doi.org/10.1109/JSTARS.2022.3166398>, 2022.
- 275 YSI Inc: Exo User Manual, Yellow Springs, 1–154 pp., 2017.